Journal of Experimental Botany, Vol. 60, No. 2, pp. 679–695, 2009
doi:10.1093/jxb/ern312 Advance Access publication 16 December, 2008
This paper is available online free of all access charges (see http://jxb.oxfordjournals.org/open_access.html for further details)

Journal of Experimental Botany
www.jxb.oxfordjournals.org

RESEARCH PAPER

Influence of *clavata3-2* mutation on early flower development in *Arabidopsis thaliana*: quantitative analysis of changing geometry

Tomasz Szczęsny[1], Anne-Lise Routier-Kierzkowska[1] and Dorota Kwiatkowska[2,*]

[1] Institute of Plant Biology, University of Wrocław, Kanonia 6/8, 50-328 Wrocław, Poland
[2] Department of Biophysics and Morphogenesis of Plants, University of Silesia, Jagiellońska 28, 40-032 Katowice, Poland

Received 9 September 2008; Revised 14 November 2008; Accepted 14 November 2008

Abstract

Early development of the flower primordium has been studied in *Arabidopsis thaliana clavata3-2* (*clv3-2*) plants with the aid of sequential *in vivo* replicas and longitudinal microtome sections. Sequential replicas show that, although there is no regular phyllotaxis in the *clv3-2* inflorescence shoot apex, the sites of new primordium formation are, to a large extent, predictable. The primordium always appears in a wedge-like region of the meristem periphery flanked by two older primordia. In general, stages of primordium development in *clv3-2* are similar to the wild type, but quantitative geometry analysis shows that the *clv3-2* primordium shape is affected even before the CLAVATA/WUSCHEL regulatory network would start to operate in the wild-type primordium. The shape of the youngest primordium in the mutant is more variable than in the wild type. In particular, the shape of the adaxial primordium boundary varies and seems to be related to the shape of the space available for the given primordium formation, suggesting that physical constraints play a significant role in primordium shape determination. The role of physical constraints is also manifested in that the shape of the primordium in the later stages, as well as the number and position of sepals, are adjusted to the available space. Longitudinal sections of *clv3-2* apices show that the shape of surface cells of the meristem and young primordium is different from the wild type. Moreover, there is only one tunica layer in both the meristem and in the primordium until it becomes a bulge that is distinctly separated from the meristem. Starting from this stage, the anticlinal divisions predominate in subprotodermal cells, suggesting that the distribution of periclinal and anticlinal cell divisions in the early development of the flower primordium is not directly affected by the *clv3-2* mutation.

Key words: *Arabidopsis thaliana*, *clavata3-2*, early flower development, shoot apex, primordium geometry.

Introduction

Two fundamental processes take place at the shoot apical meristem (SAM): meristem self-perpetuation and the formation of lateral organs, like leaves or axillary shoots. In the process of self-perpetuation, the general shape and size of the SAM are maintained, despite their changes due to primordium formation. During the vegetative phase of development, the SAM of seed plants reveals a characteristic cytohistological zonation (Foster, 1939; Buvat, 1989). The central zone is the distal meristem portion, involved mainly in SAM self-perpetuation. It comprises the upper zone of initial cells (i.e. putative stem cells) and the zone of central mother cells, which is a group of cells regarded as the SAM organizing centre (Lenhard and Laux, 1999; Kwiatkowska, 2004). The rib meristem, situated beneath the central zone, contributes to the formation of internal stem tissues. The central zone and rib meristem are surrounded by the peripheral zone where lateral organ primordia are formed. The cytohistological zones differ in cell division and growth rates, both of which are the lowest in the central zone. In angiosperms the SAM can be also divided into zones that

* To whom correspondence should be addressed: E-mail: Dorota.Kwiatkowska@us.edu.pl

are defined by specific planes of cell divisions (Buvat, 1989; Romberger *et al.*, 1993). The tunica comprises surface cells in which divisions are virtually exclusively anticlinal. As a consequence, the tunica cells are arranged in one to several layers. Remaining SAM cells, i.e. the SAM corpus cells, divide both anticlinally and periclinally. Tunica/corpus zonation is characteristic for both vegetative and reproductive angiosperm SAM.

In *Arabidopsis thaliana* the cytohistological SAM zonation typical for the vegetative developmental phase is, to a certain extent, preserved in the inflorescence SAM as well (Vaughan, 1955; Laufs *et al.*, 1998; reviewed in Kwiatkowska, 2008). Moreover, in both vegetative and inflorescence SAM of *Arabidopsis*, cytohistological zones are distinguished by gene expression patterns (Brand *et al.*, 2000; Traas and Doonan, 2001). In particular, the zone of putative stem cells is the expression domain for *CLAVATA3* (*CLV3*), which together with *CLV1* and *CLV2* belongs to the *CLAVATA* gene family (Fletcher *et al.*, 1999). The organizing centre, in turn, is specified by *WUSCHEL* (*WUS*) expression (Mayer *et al.*, 1998). WUS and CLV1, 2, 3, together with other factors, are involved in the regulation of SAM self-perpetuation. CLV3 is a small protein that interacts with the CLV1/CLV2 LRR or the CLV1/CLV2-CRN receptor as a ligand–receptor complex, activating the CLV–WUS signal transduction pathway (Müller *et al.*, 2008; Ogawa *et al.*, 2008). This pathway acts in a negative feedback loop, where CLV3 limits *WUS* expression and WUS positively regulates *CLV3* expression. This way *WUS*, expressed in the organizing centre, specifies the putative stem cells located above, while the CLV3 signal negatively regulates *WUS* expression, thus limiting the size of the stem cell zone (Laux *et al.*, 1996; Fletcher *et al.*, 1999; Sharma *et al.*, 2003). WUS has also been shown to play a role in cytokinin signalling (Leibfried *et al.*, 2005; Lindsay *et al.*, 2006), which may influence cell division frequency in the SAM.

Disruption of the CLV/WUS feedback loop leads to specific SAM phenotypes. In *wus* seedlings, after the formation of a few leaves the SAM is prematurely terminated and shoot formation is continued only by the iterative appearance of adventitious axillary meristems (Laux *et al.*, 1996). In *clv* mutants, the *WUS* expression level increases leading to uncontrolled enlargement of the central zone and, as a consequence, to the enlargement of the SAM. For example, inflorescence SAM in the *clv3-1* plants is several times larger than in the wild type (Laufs *et al.*, 1998). The increase in SAM size in *clv* is often accompanied by shape changes of the fasciation type and the phyllotactic pattern generated at this SAM is also markedly changed (Clark *et al.*, 1993, 1995; Kayes *et al.*, 1998). Since the value of the mitotic index for the SAM surface cells (L1 cells) is significantly lower in *clv3-1* than in the wild type, Laufs *et al.* (1998) postulated that the role of CLV3 in SAM self-perpetuation is in regulating cell transition from the central to the peripheral zone, rather than in limiting cell division rates in the central zone. This is further supported by the observation that, even in the wild type, the size of the CLV3 domain is fluctuating on behalf of a limited number of peripheral zone cells adopting the identity of central zone cells defined by *CLV3* expression (Reddy and Meyerowitz, 2005). In SAMs with silenced *CLV3*, the number of peripheral zone cells adopting central zone identity increases and the domain of the *CLV3* promoter (*pCLV3* domain) expands, which is one of the reasons why the general size of the central zone is increased (Reddy and Meyerowitz, 2005). This phenomenon may be a manifestation of interplay between cells of the central and peripheral zones.

A negative feedback loop involving CLV3 and WUS, similar to that operating in the SAM, also contributes to the regulation of flower primordium development (Lohmann *et al.*, 2001). Generally, in *clv* and *wus* plants the flower primordium size and numbers of flower organs per whorl are increased or decreased, respectively. In *clv3-2* plants, the strong *clv3* mutant, the flower primordium dome at the stage of sepal formation (stage 3 of Smyth *et al.*, 1990) is over twice as high and 1.5-fold wider than in the wild type (Clark *et al.*, 1995). The numbers of organs in each of the four whorls are variable, unlike the stable numbers in the wild type. The increase in organ number is larger in later appearing whorls, i.e. stamens and carpels, than in the whorls of the sepals and petals (Clark *et al.*, 1995). The gynoecium is formed as a ring around a pool of still proliferating cells, in contrast to a pair of carpels and determinate growth of the flower primordium in the wild type. These undifferentiated cells may develop an additional whorl of carpels (Clark *et al.*, 1995). In *wus* flowers, by contrast, the numbers of flower organs are reduced, and flower primordium growth is prematurely terminated, so that carpels are often not formed at all (Laux *et al.*, 1996).

During the early stages of primordium formation, the SAM surface is partitioned and the geometry of the SAM periphery and the young primordium changes rapidly. Since the specification of shape can be a subject of optical illusion, for example, when scanning electron micrographs are analysed, and the geometry of both the SAM and the primordium is complex, studies of morphogenesis need to be complemented by quantification of the local geometry (Dumais and Kwiatkowska, 2002). The local geometry can be characterized by two variables: principal curvature directions and Gaussian curvature. The principal curvature directions are the directions in which curves lying on the examined surface attain either maximal or minimal curvatures. Gaussian curvature measures the overall surface curvature and shows to what extent the surface is different from the plane (Struik, 1988).

The quantification of the local geometry applied to the reconstructed shoot apex surface and obtained with the aid of the sequential replica method, has been used to analyse early flower primordium formation in the wild-type *Arabidopsis thaliana* Columbia ecotype (Kwiatkowska, 2006). The earliest developmental stage of the *Arabidopsis* flower primordium defined in this way is the initial bulging of the SAM periphery, occurring in the lateral direction (i.e. in a direction perpendicular to the stem axis). At this stage, the primordium formation site is a region of increased Gaussian curvature and is not clearly delineated from the meristem

(Kwiatkowska, 2006). The stage corresponds most likely to the 'initial stage 0' defined by Long and Barton (2000), which is distinguished by the lack of *SHOOTMERISTEMLESS* (*STM*) expression in future primordium cells (anlagen). The initial bulging stage leads to the formation of a shallow crease, a saddle-shaped region that probably represents an axil of the rudimentary bract, as confirmed by the expression patterns of *STM* and *AINTEGUMENTA* (*ANT*) (Long and Barton, 2000). The ability of the *Arabidopsis* inflorescence SAM to form the bract is revealed in mutants like *unusual floral organs* (Hepworth *et al.*, 2006). At the bottom of the shallow crease a flower primordium proper is formed later on due to bulging in an upward direction, i.e. parallel to the stem axis (Kwiatkowska, 2006). The flower buttress stage, i.e. stage 1 of the commonly used system of ontogenetic stages in *Arabidopsis* flower development introduced by Smyth *et al.* (1990), most probably begins in the course of the consecutive initial bulging stage and bulging at the shallow crease. A time lag in recognition of the first developmental stage is due to the use of different methods by Smyth *et al.* (1990) and Kwiatkowska (2006). Once the flower primordium proper has been formed, the boundary between the SAM and the primordium is well delineated. At this stage the primordium grows rapidly preserving a bulge shape (stage 2 of Smyth *et al.*, 1990). Subsequently, the first pair of sepals appears as two folds located on the lateral sides of the primordium. Soon the second pair arises on adaxial and abaxial primordium sides, while the primordium centre retains a dome shape (Kwiatkowska, 2006). This is stage 3 of Smyth *et al.* (1990).

The processes of SAM self-perpetuation and flower primordium formation are postulated to depend one on the other. Some of these interactions may be explained by a putative signalling from the central zone. The signalling depends on the zone size and influences genes involved in primordium formation (Golz and Hudson, 2002). This interdependence is manifested, for example, in that the induced increase of CLV3 level leads not only to the decrease and eventual termination of the SAM but also to a decrease in the putative repellence between the central zone and the newly formed primordia (Müller *et al.*, 2006). One of the open questions is whether the decrease in CLV3 level affects the early stages of flower formation.

CLV3 and WUS start to operate in the distal portion of flower primordium after the primordium has been separated from the SAM (stage 2). In particular, *WUS* mRNA has been detected in stage 1 flower primordia, in a small group of centrally located cells that includes the corpus cells (L3) underlying L2; while *CLV3* mRNA appears at stage 2, in L1 and L2, and persists through stage 6 (Mayer *et al.*, 1998; Fletcher *et al.*, 1999). There is, therefore, a lag lasting from the onset of primordium formation to its separation from the SAM, when the primordium development may not be directly affected by the *clv3* mutation. This makes flower development in the *clv3* mutant suitable for addressing two questions related to flower morphogenesis: the first is whether the malfunction in SAM self-perpetuation affects the earliest stages of formation of the flower primordium, and the second is on the direct effect of this mutation on flower primordium geometry, taking place later on in flower development when the CLV/WUS is expected to start to operate *de novo*. In the present study these two questions are addressed. In particular, the geometry changes of the *clv3 Arabidopsis* flower primordium during the earliest developmental stages are quantitatively analysed and compared with the data on flower development already known for the wild type. In addition, a full description of the already partly known direct effect of the *clv3* mutation on flower geometry is provided.

Materials and methods

Plant material and growth conditions

The seeds of *Arabidopsis thaliana clavata3-2* on the Landsberg *erecta* (L*er*) background, here called *clv3-2*, were obtained from Professor Rüdiger Simon (H Heine University of Düsseldorf). Potted plants were grown in short days (10/14 h day/night) throughout the experiment, with illumination of 9 W m^{-2}, and temperature ranging from 20 °C (night) to 28 °C (day).

Data collection

Inflorescence shoot apices of *clv3-2* plants were studied with the aid of a non-destructive sequential replica method (Williams and Green, 1988; Williams, 1991). Data were collected the same way as described by Kwiatkowska (2006). Briefly, sequences of replicas (dental polymer moulds) were taken from individual apices at 12 h intervals for 24–36 h. Next, epoxy resin casts prepared from these moulds were sputter-coated and observed by scanning electron microscopy (SEM) LEO435VP. For each apex two SEM micrographs were taken, one tilted by 10° with respect to the other, in order to facilitate the stereoscopic reconstruction.

The replicas were taken from plants 7–8 weeks after seed germination, when the inflorescence axis length was between 2–10 mm and before the oldest flower buds opened. Sequences of replicas were obtained from six *clv3-2* apices. In these sequences, the morphogenesis of 18 flower primordia representing different developmental stages was studied. In addition, the apical portions of 14 inflorescence shoots were collected from *clv3-2* plants growing in the same conditions, in order to prepare microtome sections of shoot apices.

In order to compare the data obtained for the mutant with wild-type *Arabidopsis*, the previously collected data for *Arabidopsis* ecotype Columbia were used (as described by Kwiatkowska, 2006). Replicas were also taken from five exemplary apices of a Landsberg *erecta* (L*er*) ecotype, since this is the background for *clv3-2*. All these plants were grown in pots, with the same temperatures and illumination as the *clv3-2* plants throughout the experiment, but in long days (16/8 h day/night). The replicas were taken from these apices 5 weeks after germination, when the length of

the inflorescence axes varied between 4 mm and 40 mm (Kwiatkowska, 2006).

Quantitative analysis

Quantitative analysis of the collected data comprised two steps: the stereoscopic reconstruction and geometry quantification. For the stereoscopic reconstruction step a recently described protocol was used (Routier-Kierzkowska and Kwiatkowska, 2008), while the protocol for the second step, i.e. the geometry quantification, was the same as that described earlier by Dumais and Kwiatkowska (2002). Computer programs used for this analysis have been written in Matlab (The Mathworks, Natick, MA, USA) and are available from the authors upon request.

The new stereoscopic reconstruction protocol is based on an automatic dense matching of the two stereo micrographs taken from each replica, followed by a triangulation step (Routier-Kierzkowska and Kwiatkowska, 2008). This procedure allows the smooth surface of the replica to be reconstructed and takes into account slight differences in magnification between the two micrographs which could lead to erroneous three-dimensional reconstructions. Cell outlines, i.e. their connected vertices, are digitized on one of the micrographs, and projected on the reconstructed 3-D apex surface, resulting in a spatial reconstruction of the cell surfaces. These coordinates of the vertices are then used for the curvature computations. Because the shape of the *clv3-2* inflorescence shoot apices is unusually complex, the reconstructions of the *clv3-2* flower primordium surface have not allowed the computation of the growth rates to be performed, as has been done earlier for the wild type (Kwiatkowska, 2006). This was because it was necessary to observe the primordia in the SEM chamber with a large span of tilt angles, which possibly influenced the absolute magnification values. Therefore, quantitative analysis was limited to geometry computation and the assessment of growth only by means of the Cumulative Mitotic Index (CMI) (Reddy *et al.*, 2004).

The shape of the flower primordium surface was quantified by means of principal curvature directions and Gaussian curvature. These variables have been computed for every surface approximating a group of vertices of a given cell and its direct neighbours, i.e. not for the outer periclinal walls of single cells (Dumais and Kwiatkowska, 2002). In the case of cells located at the margin of the studied apex region, the curvature variables have been computed only if a cell has at least five neighbours. In the figures, the principal curvature directions are represented by crosses. Cross arms point to the principal curvature directions and arm lengths are proportional to the given curvature values. The Gaussian curvature is presented in the colour maps.

The reconstructed apex surfaces were also used to compute the surface areas of the outer cell walls, in order to compare cell sizes of the SAM and flower primordia representing different developmental stages. Next, on the basis of clonal analysis, the cells and their progeny were recognized in consecutive images of the same apex. This enabled estimation of CMI for every 12 h interval between consecutive replicas.

Dense reconstructions of the replica surface were then used to produce side views of the apices. In order to compare the side views of consecutive replicas taken from the same apex, the reconstructions had to be properly aligned. One way to do this is to fix the position of a selected reference region of the meristem, with the remaining apex portion 'moving freely' with respect to the reference region due to growth taking place over a given time interval. Such a reference region was chosen to be a group of 7–10 cells of the meristem surface, which were not dividing during the time interval being considered and which were situated just above the growing primordium. The two consecutive reconstructions of the given apex have to be rotated and translated so that the position of the reference region remains fixed. The rotation and translation were computed in such a way that the reference cell centres on the second reconstruction were as close as possible to the cell centres on the first reconstruction. This was achieved by minimizing the sum of squared pairwise distances between the cell centres, using a singular value decomposition approach (Arun *et al.*, 1987). The application of such a rotation to the two consecutive reconstructions allowed them to be analysed under the same angle of view.

In order to enable a comparison between development of flower primordium in *clv3-2* plants and in wild-type *Arabidopsis* mentioned above, the new reconstruction protocol was also applied to SEM images of the wild-type Columbia plants obtained earlier (previously, the stereoscopic reconstruction had been performed for these images with the protocol described by Dumais and Kwiatkowska, 2002). The same analysis has been performed for the exemplary L*er* apices. These reconstructed surfaces were used to obtain side-views of the inflorescence SAM and flower primordium surface. The CMI has also been estimated for the same wild-type sequences of replicas.

Paraffin sections and light microscopy

The apical parts of *clv3-2* shoots were fixed in FAA (5 ml 40% formalin, 5 ml acetic acid, 90 ml 50% ethanol) for 24 h, dehydrated in an ethanol series, and embedded in paraffin. Longitudinal sections of inflorescence shoot apices, 6 μm thick, were prepared with the aid of a Leica RM 2135 microtome. The sections were stained in Fast Green (Johansen, 1940), covered in Euparal (Roth), and photographed under an Olympus light microscope with the aid of an Olympus Camedia C-7070 wide zoom digital compact camera.

Statistics

Analysis of variance (ANOVA) was performed for values of cell areas on the *clv3-2* inflorescence SAM periphery and flower primordium surface at consecutive developmental stages. This was followed by a multiple comparison of means using Tukey's HSD test for unequal sample sizes. Statistica (Statsoft Inc.) software was used for this analysis.

Results

Formation sites of new flower primordia at the clv3-2 *inflorescence SAM*

The shape of the *clv3-2* inflorescence SAM is variable (compare apices in Fig. 1A and D), very complex, and does not exhibit rotational symmetry (Fig. 1). The SAM surface is usually folded, but the distribution of bumps and creases with respect to cells is often changing in time (Kwiatkowska and Szczęsny, 2004).

New flower primordia are formed at the *clv3-2* SAM periphery not observing any phyllotactic pattern. Despite this irregularity, the sites of their formation are, to a large extent, predictable. The new flower primordium always arises in a wedge-shaped portion of the SAM periphery, between two older primordia that are still in direct contact with the SAM through the already formed axils, and whose developmental stages are preceding the sepal formation (e.g. at sites indicated by arrows in Fig. 1). A new primordium was observed in every such defined SAM periphery portion examined. Often a number of primordia were formed almost simultaneously, each one in a different wedge-like SAM portion (Fig. 1A, B).

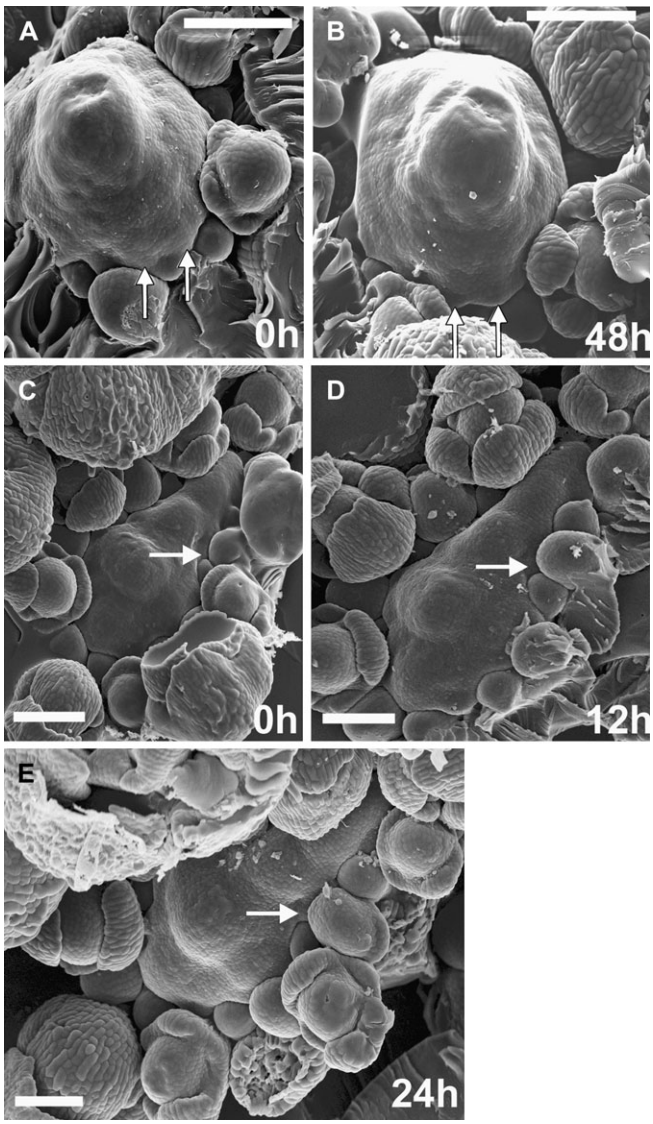

Fig. 1. Scanning electron micrographs of consecutive sequential replicas of two *clv3-2* inflorescence shoot apices (A, B and C–E) showing sites of new flower primordium formation. The same flower primordia are pointed by arrows on consecutive micrographs. Time at which the replicas were taken is given in the lower right corner of each micrograph. Bars=100 μm.

Early development a of clv3-2 *flower primordium: changes in the primordium geometry*

Before analysing changes in primordium geometry it is convenient to describe the curvature of several characteristic shapes that a primordium may resemble (Fig. 2). A surface of nearly hemispherical bulge (Fig. 2B), at every point, is convex in all directions. Thus, the plots of its principal curvature directions are crosses with nearly equal arms and the curvature in these directions is positive, while the Gaussian curvature (a product of the principal curvatures) is almost uniform and positive on the whole surface. Another type of bulge resembles a cone-like structure, the tip having been replaced by a cap (Fig. 2A). Its curvature is different at different points on the surface, although the Gaussian curvature is positive everywhere. On the sides of the cone the directions of maximal curvature are meridional (perpendicular to the axis). There is a big difference between the maximal and minimal curvatures. On the cap part, the

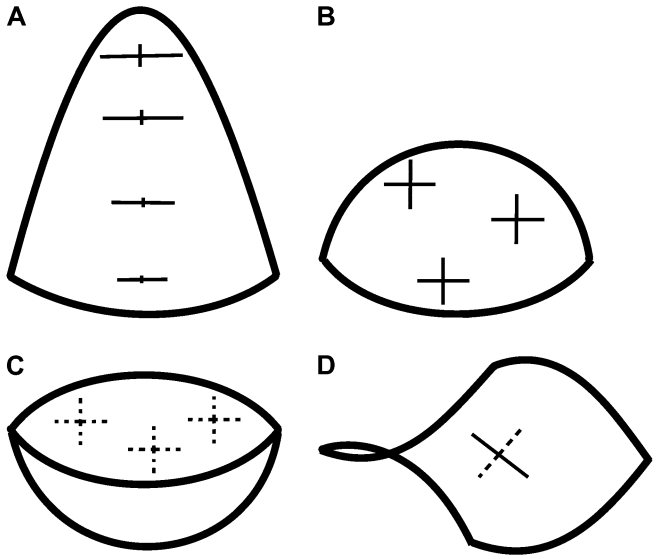

Fig. 2. Schematic surfaces representing different shapes exhibited by the flower primordium during its development: cone-like structure in which the tip of a cone is replaced by a rounded cap (A); nearly hemispherical shape (B); cavity-like shape (C); crease (D). Exemplary crosses, plotted on the surfaces, represent the principal directions of curvature. Cross arm lengths are proportional to the curvature in a given direction. The arm is plotted as a solid line if, in this direction, the surface is convex, and as a dashed line if it is concave.

curvatures in the principal curvature directions are all similar to each other, while the value of the Gaussian curvature is elevated. A cavity-like surface (Fig. 2C) also has positive Gaussian curvature, but at every point it is concave in all directions and both the principal curvature values are negative. The last type of shape, a crease, resembles a saddle and is characterized by negative Gaussian curvature (Fig. 2D). At every point it is convex in one principal direction and concave in the other, meaning that the values of the principal curvatures are of opposite signs.

The shape of the periphery of the *clv3-2* inflorescence SAM is very complex (Fig. 1). Therefore, in order to recognize the earliest stages of flower primordium formation the fate of a given periphery region needs to be followed in consecutive replicas of the same apex (compare P1 in Fig. 3A, E with B, F; P1 in Fig. 4A, G with C, I). Note that, in order to enable observation of young primordia in SEM, older primordia were dissected from the epoxy resin casts of these apices.

The earliest recognized site of primordium formation is convex, of a positive Gaussian curvature, generally higher than in adjacent SAM regions (P1 in Fig. 3). The curvature values in the principal curvature directions are usually similar to each other. During this stage, also referred to as initial bulging, the primordium surface seems to bulge in a lateral direction, i.e. in a direction away from the stem axis. The value of the Gaussian curvature at the primordium formation site gradually increases for at least 12 h (compare P1 in Fig. 3C and D).

The initial bulging leads to the formation of a shallow crease (Fig. 4). Then the adaxial primordium portion (adjacent to the SAM), which is visible in the top view of the apex, is characterized by low, often negative, Gaussian curvature. This portion of the primordium surface is concave, mainly in the direction perpendicular to the SAM margin (P1 in Fig. 4D–F and G–I). In many cases, a cavity-like region appears within the shallow crease (as within the crease between P1 and SAM in Fig. 4F). As mentioned above, such a region is concave in all directions and is characterized by high positive Gaussian curvature. The shallow crease is maintained for at least 24 h (Fig. 4A–F).

The stage of initial bulging, i.e. the shallow crease formation, resembles the first flower developmental stage in the wild type (compare P1 in Fig. 3F with P1 in Fig. 3G). However, in the mutant, there are often cavity-like regions within the shallow crease, which is not the case in the wild type (compare P1 in Fig. 4I with P1 in Fig. 4J). Also, the sizes and shapes of individual primordia in *clv3-2* are variable (compare, for example, P3 in Fig. 3A with P1 in Fig. 4A), unlike in the wild type.

During the following 12–24 h, the primordium surface starts to bulge upward (Figs 5, 6). The abaxial part of the shallow crease changes its shape to convex (compare P1 in Fig. 5C, E with D, F). Simultaneously, on the adaxial side of the primordium, a crease-like boundary between the primordium and the SAM becomes distinct. This is a band, 2–5 cells wide, concave across the SAM margin (Figs 5B, D, 6B, D). In this respect the boundary in *clv3-2* is similar to the wild type. However, the mutant boundary attains various shapes. In some cases it seems much more distinct at its centre than at the sides. This is because in the centre there is a cavity-like region between the SAM and the young primordium (compare P1 in Fig. 5C–F with P1 in Fig. 5G). In other cases the boundary depth and distinctness is more uniform along the SAM–primordium boundary (Fig. 6C–F). At this stage, the SAM slopes adjacent to the primordium are often very steep which makes the primordium appear shelf-like (Fig. 6F).

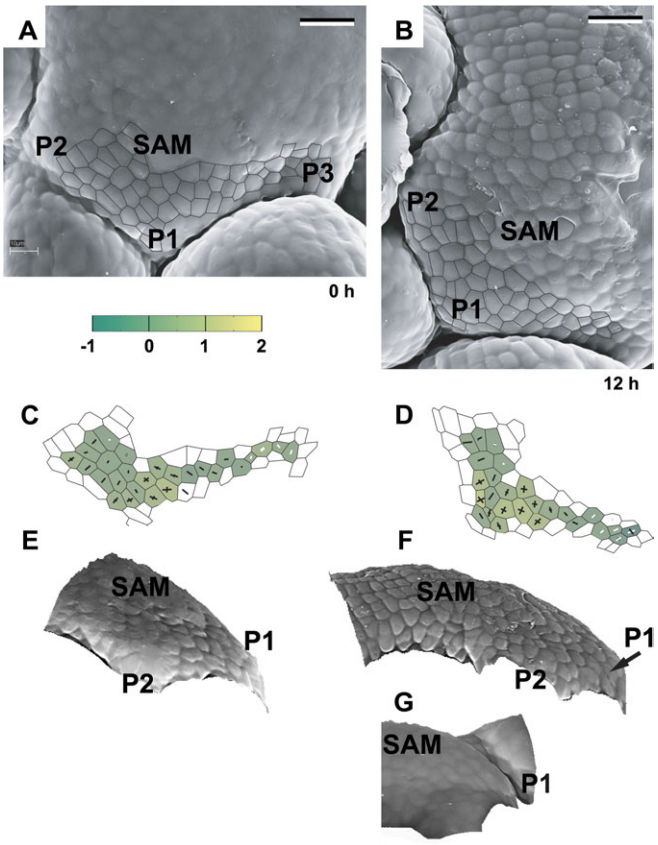

Fig. 3. The developmental sequence showing the earliest detectable stages of primordium formation at the SAM periphery. Scanning electron micrographs (A, B), curvature plots (C, D), and side views of the reconstructed surface (E, F) were obtained from sequential replicas of the periphery of the *clv3-2* inflorescence shoot apex No. 1. The side view of the reconstruction shown in (G) was obtained from the replica of the L*er* inflorescence shoot apex. The time at which the replica was taken is given in the lower right corner of each micrograph. Cell outlines are overlaid on the micrographs for the region represented in the curvature maps. The colour map represents Gaussian curvature, while cross arms point to the curvature directions. Gaussian curvature is given in 10^{-3} μm^{-2}. The length of cross arms is proportional to the curvature value in this direction. Arm appears in white if, in this direction, the surface is concave. A black arm points to the convex directions. The shoot apical meristem is labelled as SAM. Flower primordia are labelled by P. Primordia P1 and P2 are at the beginning of the initial bulging developmental stage. Bars=20 μm.

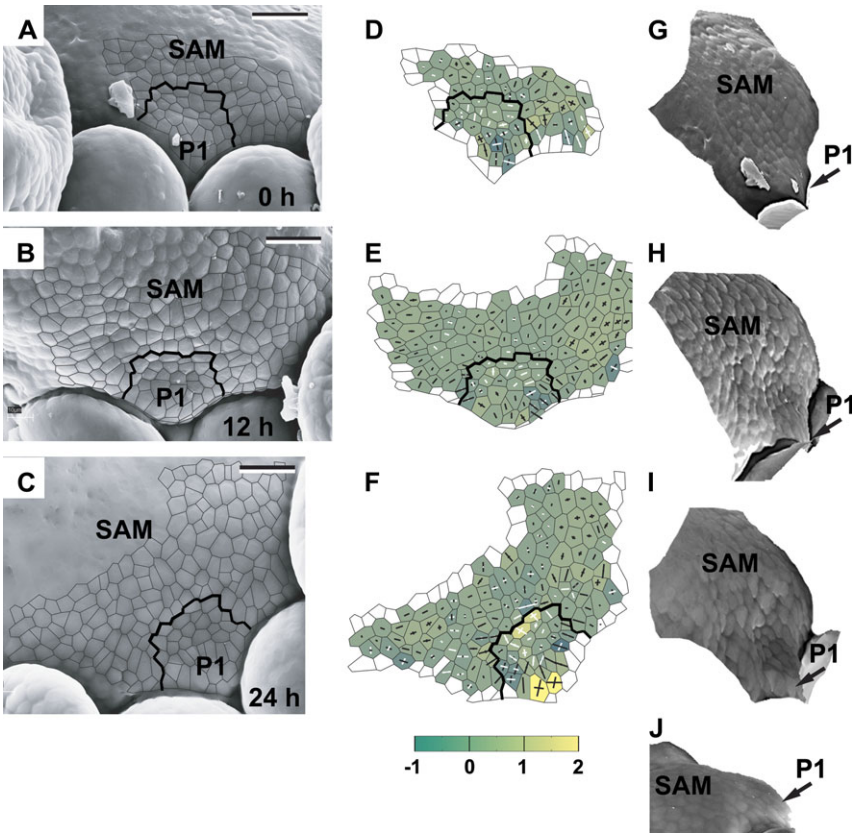

Fig. 4. The sequence showing the flower primordium that has attained a shallow crease shape. The development of this primordium is somewhat more advanced than that of primordia P1 and P2 shown in Fig. 3. Scanning electron micrographs (A–C), curvature plots (D–F), and side views of the reconstructed surface (G, J) show the periphery of the *clv3-2* inflorescence shoot apex No. 2. The side view of the reconstruction shown in I was obtained from the replica of the L*er* inflorescence shoot apex. Labelling as in Fig. 3. Bold black lines on the micrographs and curvature plots point to the putative boundary between the primordium P1 and the SAM recognized in the last plot of the sequence (C, F) and then backwards on the preceding plots on the basis of clonal analysis. Bars=20 μm.

Once the adaxial primordium boundary becomes distinct, the primordium remains a bulge, of a rather regular shape for more than 24 h (Figs 7–9). During this time the primordium surface area increases while the Gaussian curvature of the primordium surface remains positive (Figs 7C, D, 8C, D, 9D–F). The shape of the primordium is first more or less hemispherical (Figs 7C, 8C). Afterwards it changes into a cone-like structure covered with a cap (Figs 7D, 9D, E). While the primordium increases, the crease at the adaxial primordium boundary deepens. The shape of the cells located at the bottom of the crease is unique, i.e. they are very narrow and elongated along the crease. The outer periclinal walls of these cells are folded (see arrows in Fig. 7E and Fig. 8F).

The period in primordium development starting from the moment when its adaxial boundary becomes distinct and lasting until the onset of sepal formation closely resembles the bulge stage of the wild type (compare P1 in Fig. 7F and P1 in Fig. 7G). However, a rudimentary bract, characteristic of the wild type, could not have been detected in any of the *clv3-2* primordia examined. Moreover, in *clv3-2* apices the outline of the adaxial primordium boundary is variable. In some primordia the boundary is nearly straight (Fig. 7A, B), while in others it is of a crescent shape (Fig. 8A, B). The SAM overtops the primordium bulge (Figs 8E, F, 9G, I).

When the primordium is in the bulge stage of development, the adjacent portions of the SAM periphery attain the shape characteristic of the earliest stages of primordium formation. The sites of new primordium formation are located on both sides of the bulge (Figs 8E, F, 9A–C).

The bulge stage is followed by the formation of sepals (Figs 10, 11). In the *clv3-2* flower primordium the sepal formation sites are difficult to predict. The number of sepals is variable and usually different from four (e.g. P1 in Fig. 11A has six sepals; five sepals will most likely be formed in the primordium in the upper part of Fig. 11D). The arrangement of sepals differs from the wild type, i.e. it is uncommon that there are two pairs of opposite sepals (for example, in the primordium in Fig. 10 a single sepal arises, while the flower primordium in Fig. 11 has three pairs of sepals) and the arrangement of sepals is usually not regular (the angular distances between adjacent sepals are different for example in Fig. 11B). Moreover, the width of sepal primordia (angular size) is often variable (e.g. compare sepal primordia of P2 in Fig. 12G or I). In some cases it is very difficult to define a boundary between the adjacent sepal

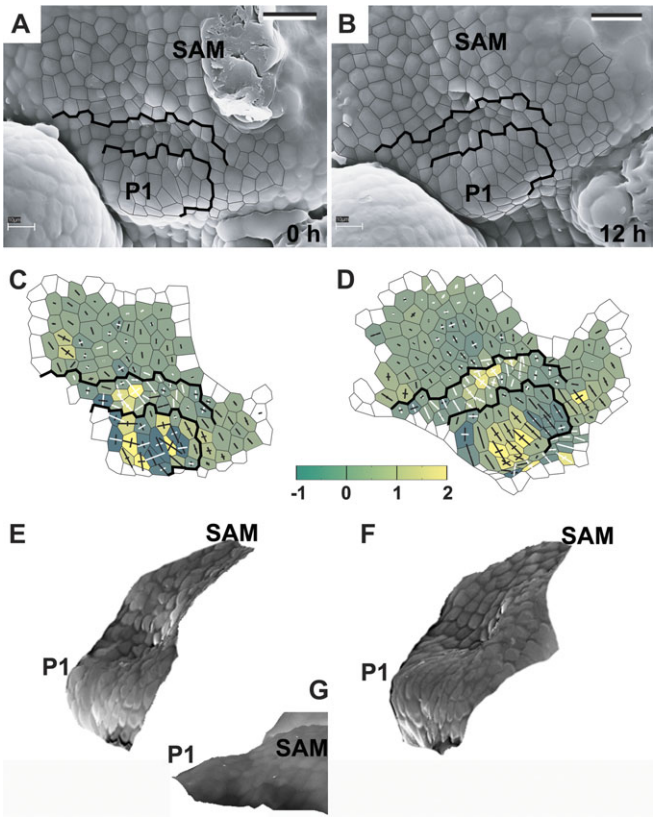

Fig. 5. Flower primordium with a portion of its surface bulging upward, i.e. switching from the shallow crease to an early bulge stage. A 'cavity' can be observed at the boundary between the primordium and the SAM. Scanning electron micrographs (A, B), curvature plots (C, D), and side views of the reconstructed surface (E, F) show the periphery of the *clv3-2* inflorescence shoot apex No. 3. The side-view of the reconstruction shown in (G) was obtained from the replica of the L*er* inflorescence shoot apex. Labelling as in Fig. 3. Bars=20 μm.

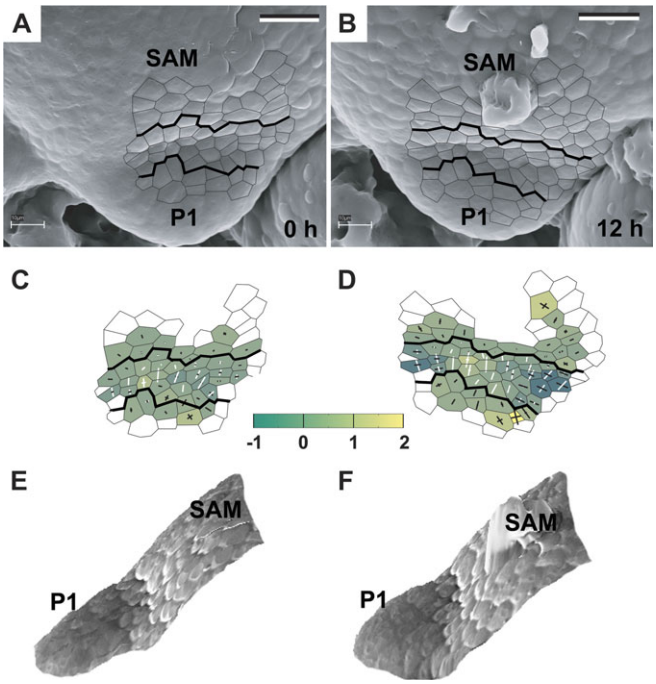

Fig. 6. Flower primordium switching from the shallow crease to an early bulge stage. Its developmental stage is similar to the primordium shown in Fig. 5, but this primordium boundary with the SAM is a slightly curved crease with no apparent cavity. Scanning electron micrographs (A, B), curvature plots (C, D), and side views of the reconstructed surface (E, F) show the periphery of the *clv3-2* inflorescence shoot apex No. 4. Bars=20 μm.

primordia, as they seem to be fused (lateral sepals in Fig. 11B). In fact, in some cases a ring-like structure presumably formed via adjacent sepal fusion, surrounds the flower primordium dome (Fig. 12A–E). In all the cases the development of sepal primordia on the abaxial side of the flower primordium seems to be faster than on the adaxial side (compare abaxial and adaxial sepal of flower primordium in Fig. 11A, B), similar to the wild type flowers. The remaining dome of the flower primordium maintains positive Gaussian curvature (Figs 10C, D, 11C, D), and is not overtopped even by quite large sepal primordia (Fig. 11E, F). Also, even at this stage, the flower primordium remains overtopped by the SAM (Fig. 12I–K).

The examination of developmental sequences reveals that the shape attained by a flower primordium, in particular, the shape of the primordium bulge (Fig. 12A–E, P1 in Fig. 12F) and the position and number of sepal primordia (P1 in Fig. 12G, H, P1 in Fig. 12J, K), seems to be adjusted to the available free space, which is delimited by the nearest flower primordia (younger or older), and the basal portion of the SAM. In particular, the portions where this available space contour attains a wedge-like shape seem to be preferable for the sepal formation (e.g. primordium portions indicated by an arrow in Fig. 12G, H, J, K).

Cell size during the development of the clv3-2 *flower primordium in comparison with the wild type*

In the *clv3-2* apex, similar to the wild type, cell sizes (mean cell surface areas assessed for the outer periclinal cell walls) are larger for the SAM than for the youngest flower primordium (Table 1). Starting from the bulge stage, the differences between the mutant and the wild type become apparent. The very characteristic feature of wild-type flower development is a large increase in cell size taking place at the onset of the bulge stage, while in *clv3-2* flower development, cell sizes at the bulge stage are very similar to the preceding stages. However, in the mutant, the cell size increases strongly in the following stage, i.e. during sepal formation, which again is unlike the wild type.

Cumulative Mitotic Index during flower primordium development in clv3-2 *compared with the wild type*

The value of the CMI in the earliest developmental stages of *clv3-2* flower development is much lower than during the corresponding stages of flower development in the wild type (Table 2). However, during the bulge stage, the CMI in

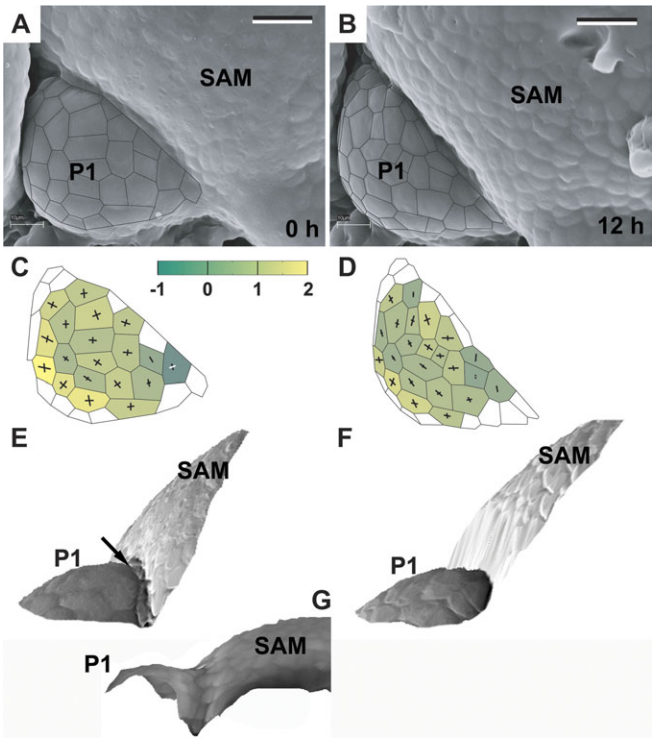

Fig. 7. Flower primordium in an early bulge stage. Scanning electron micrographs (A, B), curvature plots (C, D), and side views of the reconstructed surface (E, F) showing the portion of periphery of the *clv3-2* inflorescence shoot apex No. 4, different from the portion shown in Fig. 6. The side-view of the reconstruction shown in (G) was obtained from the replica of the L*er* inflorescence shoot apex. The arrow in (E) points to the axil cells, of which the outer walls are folded. The cellular pattern on the SAM periphery in the reconstruction (F) is missing due to the strong steepness of this SAM portion. Bars=20 μm.

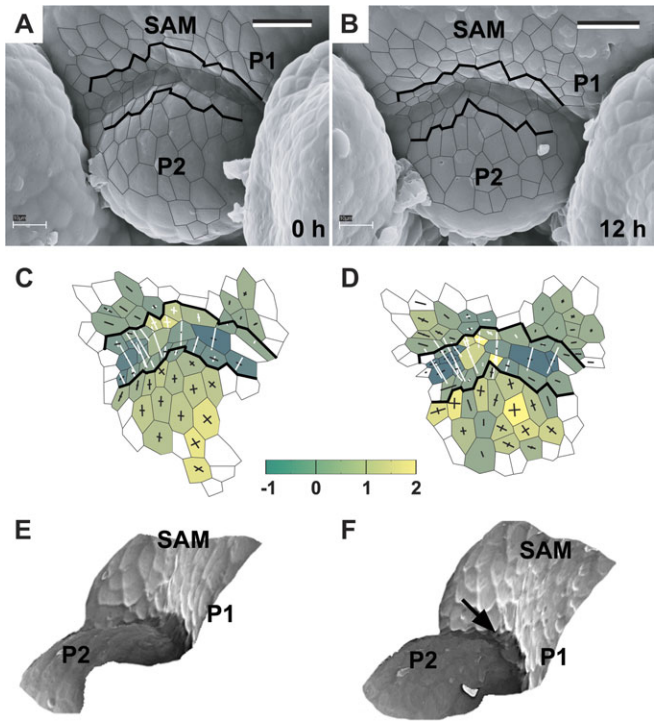

Fig. 8. Flower primordium in a medium bulge stage (P2). Scanning electron micrographs (A, B), curvature plots (C, D), and side views of the reconstructed surface (E, F) show the portion of periphery of the *clv3-2* inflorescence shoot apex No. 4, different from the portions shown in Figs 6 and 7. P1 is in the initial bulging stage. Arrow in (F) points to the axil cells, which outer walls are folded. Bars=20 μm.

clv3-2 strongly increases and becomes higher than in the wild type. In the following stage, i.e. sepal formation, the situation reverses. In *clv3-2* the CMI decreases, while in the wild type it strongly increases, becoming higher than in the preceding wild-type stage and in the sepal formation stage in the mutant.

Shape and cellular organization of the clv3-2 *inflorescence SAM and flower primordium: examination of longitudinal sections*

The shape of *clv3-2* inflorescence SAM is complex and very variable (Figs 1, 13). Thus it is difficult to obtain a precise median longitudinal section of the meristem. Since meristems are often fasciated, some of the sections probably show more than one meristem, not necessarily both in their median section (as in Figs 13A or C, where quite possibly two meristems are present: the bigger meristem in the median section, and the smaller one, indicated by an arrow, is probably not sectioned in the median plane).

The consecutive stages of flower primordium formation described above, can also be recognized in the longitudinal sections. The flower primordium in the stage of the shallow crease, sectioned in a plane perpendicular to the shallow crease, is represented by P1 in Fig. 14A and B. P1 in Fig. 14C represents the stage of upward bulging at the bottom of the shallow crease or early bulge. Primordia in Fig. 14D–H are all in the bulge stage, arranged according to increasing size. They are all sectioned in the median plane. Note, that their shapes are different. Primordium P1 in Fig. 14E is nearly hemispherical. The top of P2 in Fig. 14F is flattened, unlike P2 in Fig. 14G, which is the cone with a cap. Starting from Fig. 14I the stages of flower organ initiation are represented.

Longitudinal SAM sections (Fig. 13) show the distinct surface layer of protodermal cells where cell divisions are exclusively anticlinal. However, in subprotodermal cells not only anticlinal but also periclinal divisions occur both in the distal and in the proximal portions of the meristem (Fig. 13A–C), as well as at the putative sites of new flower primordium formation (Figs 13, 14A, B). Thus only one tunica layer is present in *clv3-2* inflorescence SAM, unlike the wild-type inflorescence SAM where there are two tunica layers (Fig. 15F).

A single tunica layer is also apparent in flower primordia at the putative shallow crease stage (Fig. 14B) and in primordia that have just been separated from the SAM by a crease visible in a longitudinal section (Fig. 14C, D). However, during the bulge stage, subprotodermal cells

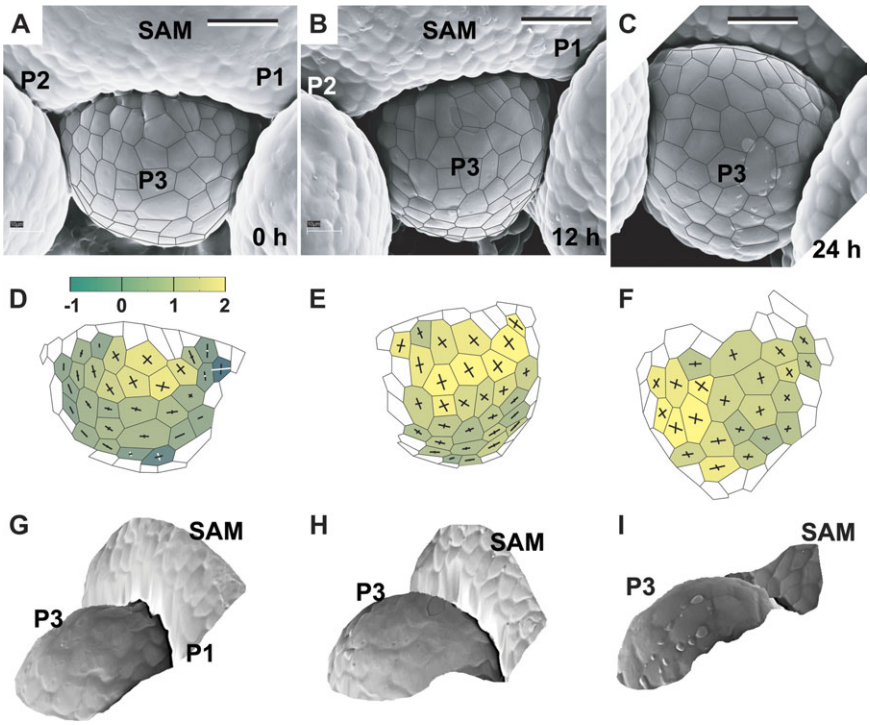

Fig. 9. Flower primordium in a late bulge stage (P3) and the adjacent two primordia exhibiting the shallow crease shape (P1 and P2). Scanning electron micrographs (A–C), curvature plots (D–F), and side views of the reconstructed surface (G–I) show the portion of the periphery of the *clv3-2* inflorescence shoot apex No. 1, different from the portion shown in Fig. 3. Bars=20 μm.

divide mostly anticlinally, at least in a major portion of the primordium surface (Fig. 14E,F), although some periclinal division in the subprotodermal cells can still be found (shown by arrows in Fig. 14). In the following developmental stage, periclinal divisions in subprotodermal cells take place in the primordium regions where the sepals are formed (Fig. 14I, J). Also at this stage, anticlinal divisions predominate in subprotodermal cells in the distal portion of the primordium, often at least up to stamen and carpel formation (Fig. 14K, L).

Cell morphology in the *clv3-2* inflorescence SAM is not uniform (Fig. 13). Firstly, cell size and degree of vacuolation increase with distance from the SAM surface. Cells located near the surface, i.e. in an outer SAM portion, up to two or three cells deep, are relatively small and slightly vacuolated. Internal cells located deeper are, in turn, much larger and more strongly vacuolated. Secondly, there are prominent differences in cell shape. The protodermal cells (the tunica layer) are generally elongated in the direction normal to the SAM surface, i.e. the tunica cell thickness is relatively big, while cell width is small. This difference is especially large in the proximal SAM portion. By contrast, small subprotodermal cells are nearly isodiametric, while the inner large cells are elongated, generally along the stem axis.

In the case of the flower primordium, the differences in cell morphology become prominent later in flower primordium development. Starting from the late bulge primordium, the centrally located cells are distinctly larger and more vacuolated than the outer cells (Fig. 14F, H). These differences become greater when the sepal, stamen or carpel primordia are formed (Fig. 14I, L). The shape of the surface layer cells differs from the internal cells only at the earliest stage of flower development. Similar to the SAM tunica cells, these surface primordium cells are elongated in the direction normal to the primordium surface, while internal cells are isodiametric (P1 in Fig. 14A, B). In primordia separated from the SAM by a distinct crease, all the cells, including the surface cell layer, are nearly isodiametric. Differences in cell shape again appear during the sepal formation stage, when the large internal cells mentioned above are elongated along the peduncle, while the remaining cells are nearly isodiametric (Fig. 14I–L).

It is striking that the shape of the new primordium, as seen in the longitudinal apex section, virtually fills all the space available between the SAM periphery and the older flower primordia. This is true from the earliest recognizable stage of flower development. Primordia P1 in Fig. 14A or B, representing the shallow crease stage, are 'filling' the space between the SAM and P2. Also P2 in Fig. 14D, which is in the bulge stage, fits between P3 and the SAM periphery where P1 emerges, similar to P2 in Fig. 14G, fitting between P3 and P1. Moreover, the shapes of sepal primordia, formed in the following stage, are adjusted to the available space, like adaxial sepals of primordia shown in Fig. 14I, J. It should be kept in mind that such relationships between flower primordium shape and available space may not always have been apparent in SEM micrographs, because older flower primordia need to be dissected from the epoxy casts of apices in order to enable observation of earlier flower developmental stages.

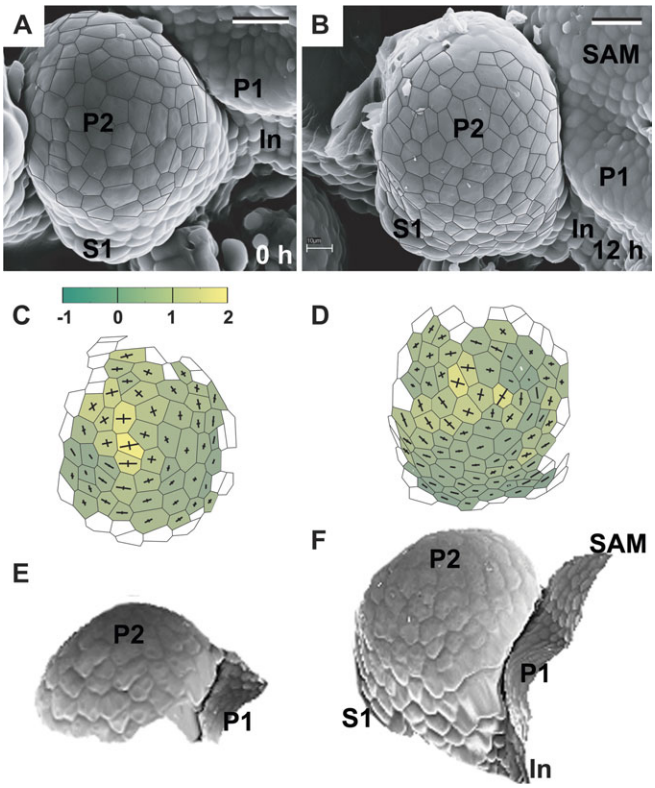

Fig. 10. Flower primordium in a sepal formation stage. Scanning electron micrographs (A, B), curvature plots (C, D), and side views of the reconstructed surface (E, F) show the portion of periphery of the *clv3-2* inflorescence shoot apex No. 3, different from the portion shown in Fig. 5. Sepal primordium (S1) and a putative internode surface (In) are labelled. Bars=20 μm.

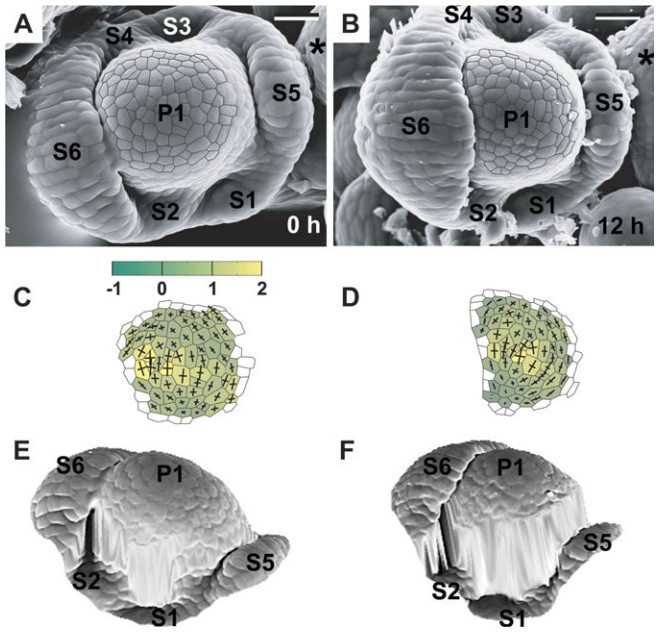

Fig. 11. Flower primordium in which six sepals have been formed. Scanning electron micrographs (A, B), curvature plots (C, D), and side views of the reconstructed surface (E, F) show the portion of periphery of the *clv3-2* inflorescence shoot apex No. 2, different from the portion shown in Fig. 4. Sepal primordia (S1–6) and the meristem (*) are labelled. The cellular pattern on the primordium periphery in the reconstruction (F) is missing due to the strong steepness of this primordium portion. Bars=20 μm.

Discussion

Early stages of flower development in clv3-2 *compared to the wild type*

The main stages in early flower primordium development in the *Arabidopsis* wild type are: (i) initial bulging leading to the shallow crease formation (Fig. 15A); (ii) bulging at the bottom of the shallow crease (Fig. 15B, C); (iii) bulge stage (Fig. 15D); (iv) sepal formation (Fig. 15E) (Kwiatkowska, 2006). Characteristically, although mature flowers in this species, similar to other Brassicaceae members, are not subtended by bracts, a rudimentary bract can be detected in the end of the second and at the beginning of the third stage (Fig. 15C, D). This suggests that the shallow crease is in fact an axil of the bract, and the flower primordium proper arises in the bract axil (Kwiatkowska, 2008). The adaxial boundary of the flower primordium proper in the wild type is nearly a straight crease of negative Gaussian curvature. Sepals are formed at the flower primordium flanks in a regular pattern.

Kwiatkowska (2006) has analysed the early flower primordium development in the *Arabidopsis* ecotype Columbia, while the *clv3-2* plants studied in the present paper are in the L*er* background. Nevertheless, the comparison between early flower development in *clv3-2* and Columbia is acceptable for the present investigation. The analysis of exemplary L*er* shoot apices performed in the course of the present investigation has not revealed any differences between the two ecotypes in the geometry of the young flower primordia at the developmental stage studies. The close resemblance is also apparent from SEM micrographs shown by Smyth *et al.* (1990) as well as by Hempel and Feldman (1994).

In general, in *clv3-2*, the stages distinguished during early flower development are similar to those distinguished for the wild type (compare Figs 3–11 with Fig. 15). The major difference between the mutant and the wild type during the earliest developmental stages is in the unique variation of primordium geometry and size at the shallow crease stage in *clv3-2*. Moreover, during bulging at the shallow crease and at the beginning of the bulge stage, no rudimentary bract can be observed with the present method in the mutant primordium, although it is temporarily apparent in the wild-type primordium, as has been shown for the Columbia ecotype (Kwiatkowska, 2006). However, the shallow crease formed in the course of the initial bulging stage in the mutant may be an axil of a bract, as postulated for the wild type. This problem could be clarified if the patterns of gene expression in the *clv3* shoot apex at this stage, in particular that of *STM* and *ANT*, were examined.

During the following stages of flower primordium development, the major difference between the mutant and the wild type is in the shape of the adaxial primordium

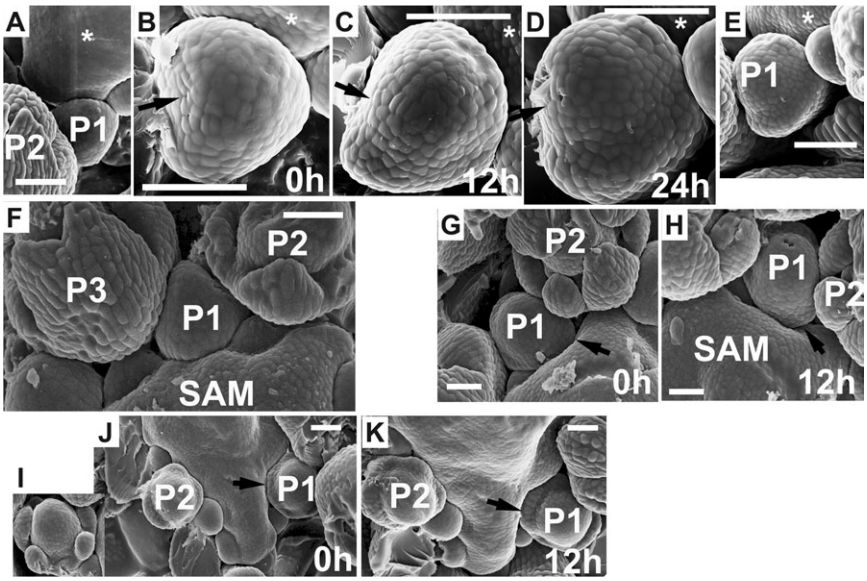

Fig. 12. Scanning electron micrographs of consecutive sequential replicas of three *clv3-2* inflorescence shoot apices illustrating the adjustment of the flower primordium bulge shape and the arrangement of sepals to the available space. Time at which the replicas were taken is given in the lower right corner of each micrograph. (A–E) Flower primordium (P1) during the sepal formation. (A) and (E) show the portion of the apex periphery where the primordium P1 is located, together with the adjacent older primordium (P2), which has been removed from replicas (epoxy resin casts) shown in (B), (C), and (D). Arrow points to the side of P1 which growth has been restricted by the P2. The asterisk labels the adaxial side of P1. (F) Flower primordium in a bulge stage (P1), the outline of which fits the space delineated by two older primordia (P2, P3) and the meristem (SAM). Note a bifurcated sepal of (P3). (G, H) Portion of the apex with flower primordium (P1); the sepal primordium (arrow) fits closely to the SAM outline. Note the increased number of sepals exhibiting various sizes in P2. (I, K) Apex with flower primordium (P1) with sepal primordia (arrow) 'filling' the space delineated by the SAM. Insert I shows a primordium with increased number of sepals, which comes from the portion of the apex not shown in J. Bars=50 μm.

Table 1. Surface areas of outer periclinal cell walls of SAM and apical part of flower primordium at different developmental stages

Values are means ±the standard error. Values of surface areas for the *clv3-2* apices, between which differences are significant at the $P < 0.05$ level of Tukey's HSD test, are indicated by different letters. Data for the wild-type apices (Col, *Arabidopsis thaliana* ecotype Columbia) included in the last column are taken from Kwiatkowska (2006). In this case all the mean values are significantly different at $P < 0.05$.

SAM or stage of flower development	Numbers of *clv3-2* apices/primordia examined	Cell surface areas in *clv3-2* (μm^2)	Cell surface areas in Col (μm^2)
SAM	3/–	41.69±0.96 a	41.79±0.40
Primordium stages			
Initial bulging (and shallow crease)	8/19	33.79±0.85 b	36.55±0.90
Bulge	3/4	39.42±1.79 a	63.16±1.37
Sepal formation	4/5	64.03±1.86 c	49.40±0.68

Table 2. Cumulative Mitotic Index (CMI) in surface cells of consecutive stages of flower primordium development in *clv3-2* and in the wild type (Col, *Arabidopsis thaliana* ecotype Columbia)

Developmental stage	CMI (% per 12 h)		Number of primordia		Number of apices	
	clv3-2	Col	*clv3-2*	Col	*clv3-2*	Col
Initial bulging (and shallow crease)	10.4	18.6	19	13	8	5
Bulge	21.6	18.5	4	6	3	3
Sepal formation	15.4	42.7	5	8	4	5

boundary. In *clv3-2* it is either crescent-shaped or nearly straight, often with a cavity in the centre, while in the wild type it is always nearly straight and no cavity has been observed (Fig. 15C, D). These variations in boundary shape in the mutant may be the consequence of a variation in the arrangement of adjacent younger flower primordia. They may be formed at various distances from the given primordium. In those cases where the younger primordia are more tightly 'packed' and the width of the given primordium base is narrower, the boundary would be more crescent-like (compare adjacent flower primordia in Figs 3 and 7).

Later on, the bulge stage is prolonged in the mutant. The bulge size is increased compared with the wild type and it attains a characteristic shape of a cone with a cap. Finally, the mutant primordium is characterized by an increased number of sepals, often by indiscrete sepal primordia, and variable sepal size.

Known effects of *clavata* mutations on flower primordium development are an increase of the primordium size and an accompanying increase in numbers of flower organs

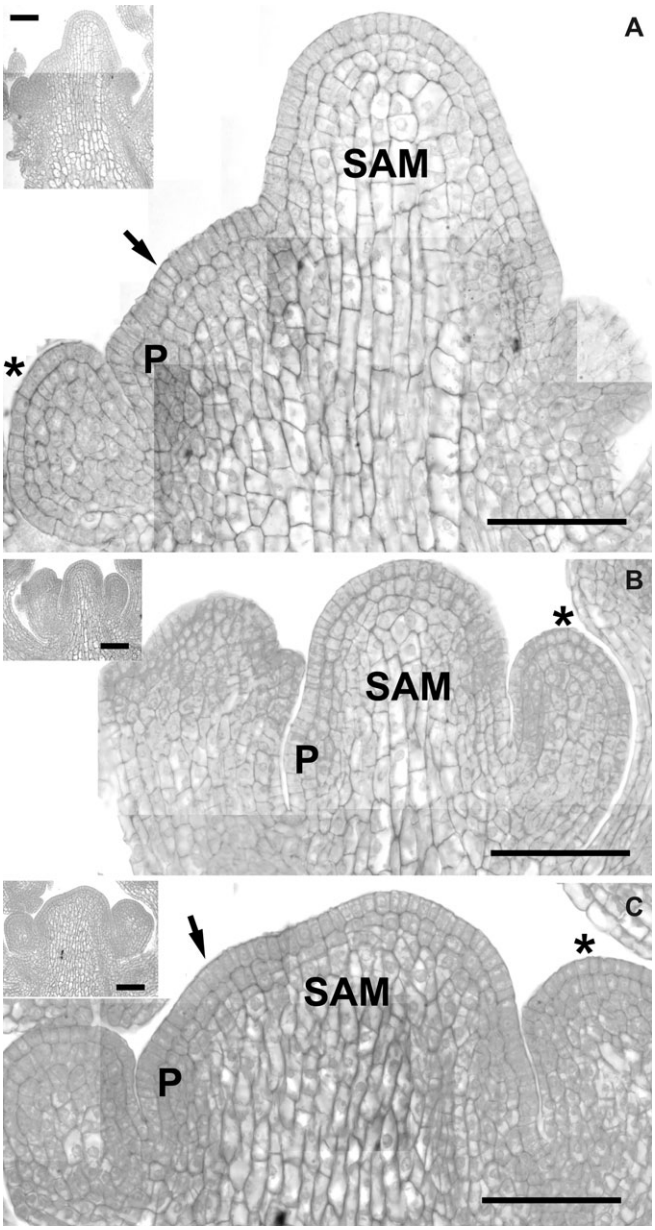

Fig. 13. Central longitudinal sections of three *clv3-2* apices. Inflorescence SAM sectioned in the median plane and the earliest stage flower primordium (P) are labelled. The arrow points to a smaller, additional meristem, appearing due to fasciation, that most likely is not in a median section (A, C). Note the characteristic shapes of SAM L1 cells as compared with L1 cells of the bulge stage flower primordium (asterisks). Insets show the overall shape of the apices. Bars=50 μm.

(Clark *et al.*, 1993, 1995). It has been also found that the *clv1-1* flowers develop slower than the wild type, meaning that flower morphogenesis is slowed down in the mutant (Crone and Lord, 1993). The increase in flower organ numbers is therefore through the changes in developmental timing, i.e. it is a heterochronic process (Crone and Lord, 1993). In particular, the extended growth of the flower primordium during the sepal formation stage accounts for the increased number of sepals. The *in vivo* study of flower primordium development in *clv3-2* presented here generally confirms the earlier observations on *clv3* (Clark *et al.*, 1993, 1995) and shows that, in *clv3-2*, similar to *clv1-1* (Crone and Lord, 1993), flower morphogenesis is slowed down. The developmental stages described last longer in the mutant than in the wild type. Also the CMI is lower and changes less dynamically during flower primordium development in *clv3-2* than in the wild type, which is a manifestation of a slower growth. In the wild type, growth rates increase rapidly at the onset of the bulge stage (Kwiatkowska, 2006), while the CMI remains similar to the earlier stages. As a consequence, in the wild type the mean cell surface area is greatly increased in the bulge stage. This is unlike *clv3-2* where, at this stage, the cell areas are similar to the preceding and following stages, while the CMI is increased. This further supports the postulate that the increased dimensions of the wild-type cells appear because the rapid cell expansion is not accompanied by rapid cell division (Kwiatkowska, 2006).

Differences in the cellular pattern of the inflorescence SAM and flower primordia visible in longitudinal sections of the *clv3-2* and wild-type apices are also prominent. In longitudinal sections, surface cells in the periphery of *clv3* SAM and surface cells of the youngest flower primordium, not yet distinctly separated from the SAM, are elongated in a direction perpendicular to the SAM surface. In SEM micrographs, these cells observed in the apex surface appear more or less isodiametric. This special shape may be due to the relatively high frequency of anticlinal cell divisions not accompanied by the adequate expansion of the meristem surface. The very striking difference between the mutant and the wild type is the restriction of the tunica to a single layer in mutant SAM and early stage primordia. What is observed in the cellular pattern is, however, the manifestation (cumulative effect) of the preceding cell divisions. In the SAM, the effects on cellular pattern are cumulative, starting from embryonic development. The single layer tunica may result from the acropetal shift of the WUS domain in the mutant, known to occur already in the embryo (Brand *et al.*, 2000; Sharma *et al.*, 2003). The domination of anticlinal divisions in the subprotodermal cells is restored at the early bulge stage of flower primordium development, when the direct effect of the *clv3* mutation is expected. This may be because, in *Arabidopsis thaliana*, as in the majority of dicots, periclinal divisions accompanying flower primordium formation are typically in L3 of the inflorescence shoot apical meristem while protodermal and subprotodermal cells divide mainly anticlinally (Vaughan, 1955; Romberger *et al.*, 1993). Such a cell division pattern is apparently preserved in the mutant, indicating that CLV3 does not play a direct role in the maintenance of the tunica/corpus organization.

In the *clv3-2* mutant, the level of *WUS* expression is elevated, which has an effect on *ARABIDOPSIS RESPONCE REGULATOR* (*ARR*), negatively regulated by WUS in the wild type. It is known that the inhibition of ARR activity, for example, in *arr* plants, leads to increased sensitivity to cytokinins (Leibfried *et al.*, 2005). Lindsay

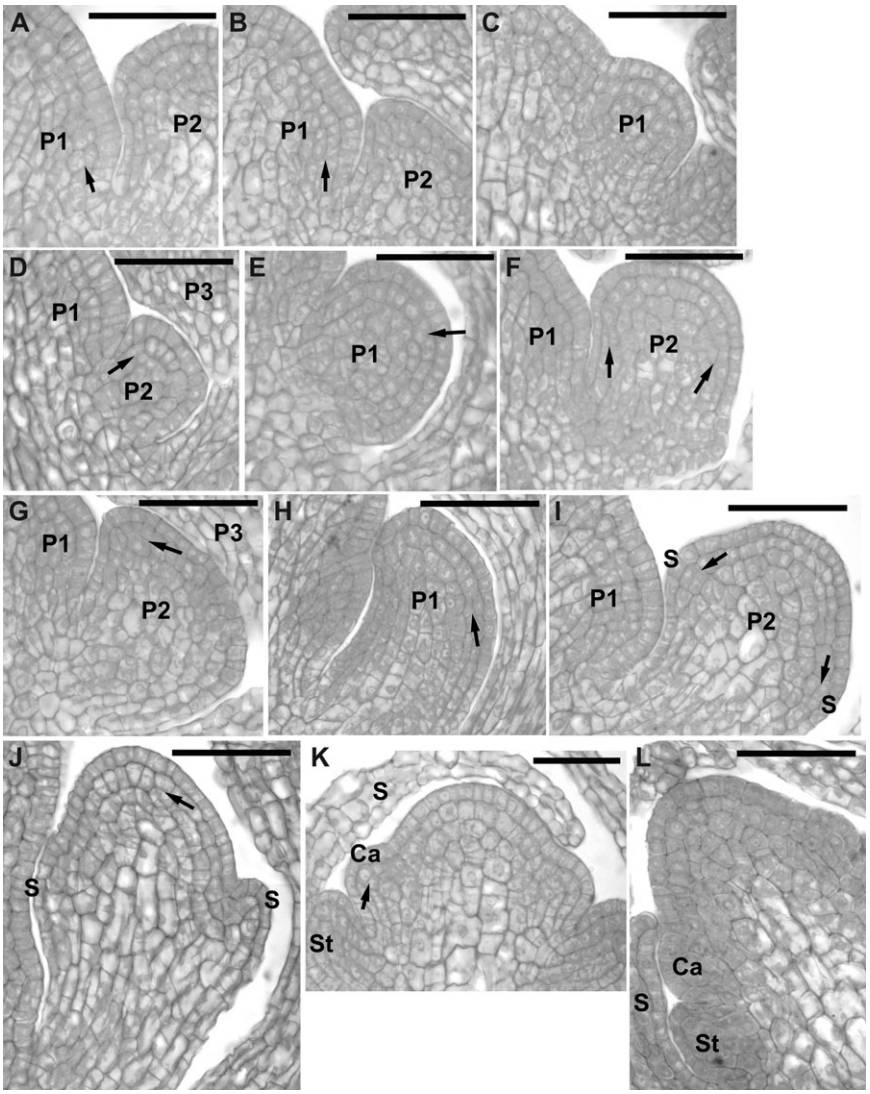

Fig. 14. Central longitudinal sections of *clv3-2* flower primordia at consecutive developmental stages. (A, B) Initial (lateral) bulging of the SAM periphery. (C) Upward bulging at the bottom of a shallow crease. (D, E) Bulge with a deep and sharp crease at the adaxial primordium boundary. (F, H) Bulge-shaped primordium 'filling' the available space between older primordia and the SAM. (I, J) Sepal formation stage. (K, L) Primordia in which stamens (St) and carpels (Ca) are formed. The flower primordia are covered by young sepals (S). The periclinal divisions in subprotodermal cells are indicated by arrows. Flower primordia are labelled with (P) and a number. Bars=30 μm.

et al. (2006) have shown that the effect of exogenous cytokinin on the SAM is similar to the *clv1-1* mutation. Also, in the inflorescence SAM of *clv1-1* plants, the level of dihydrozeatin is 9-fold higher than in the wild type. It may thus be expected that cytokinins are involved in the effect of the *clv3-2* mutation, which is known to be stronger than the effect of *clv1-1*, on the cell division pattern.

Effect of clv3-2 *on early flower development and relationships between SAM self-perpetuation and the formation of primordia*

The CLV/WUS feedback system is operating in the flower primordium, similar to the SAM, but in the flower, WUS is also negatively regulated by the AGAMOUS pathway, which is at least partially independent of the CLV pathway (Brand *et al.*, 2000; Lohmann *et al.*, 2001). The *CLV3* expression in the wild type starts at stage 2 defined by Smyth *et al.* (1990; Fletcher *et al.*, 1999; Brand *et al.*, 2000), i.e. after the primordium has been well separated from the SAM, which most probably corresponds to the bulge stage as distinguished by the aid of geometry analysis. Therefore, when interpreting the influence of the *clv3* mutation on flower development, direct and indirect effects need to be distinguished. The disturbance in the negative WUS regulation system plays a direct role in flower formation regulation, only starting from the bulge stage, and no direct effect of the *clv3* mutation can be expected in the earlier developmental stages. During this time, however, the primordium formation is apparently affected indirectly,

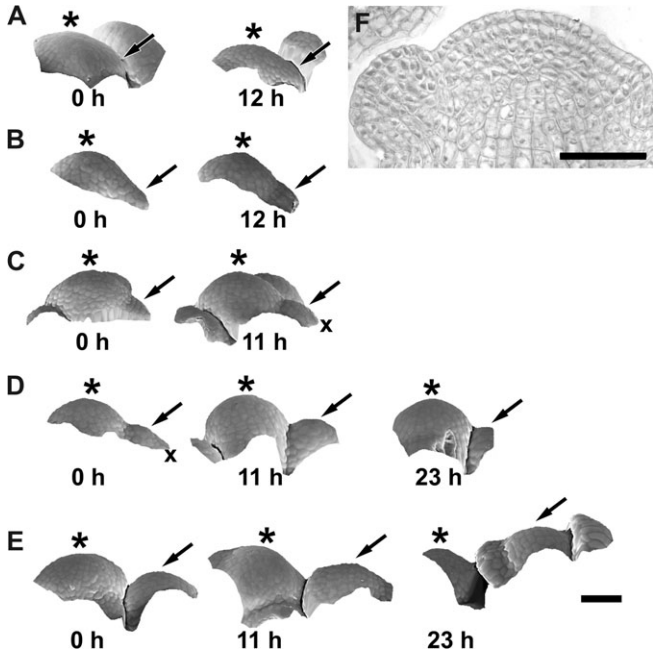

Fig. 15. Side views of the reconstructed surfaces of sequential replicas of wild-type *Arabidopsis* (Columbia) apex, showing consecutive stages of flower primordium formation (A–E), and an exemplary median section of the wild-type apex (F). Each row represents side views of an individual shoot apex. The time at which replicas were taken is given below each reconstructed surface. (A) Initial lateral bulging of the meristem periphery leading to the shallow crease formation (arrow). (B) Early stages of bulging at the bottom of the shallow crease. (C) Later stage than shown in (B): note the rudimentary bract (x) that is a tiny lateral protrusion at the abaxial side of the primordium. (D) Bulge stage. Note that the initially apparent rudimentary bract (x) disappears. (E) Sepal formation stage. The flower primordium is always indicated by an arrow, the SAM by an asterisk. Bars=40 μm.

suggesting that flower development is under the influence of the disturbed self-perpetuation of the SAM.

The present study indicates that the *clv3-2* inflorescence SAM is especially enlarged and its geometry is severely affected, which is in accordance with the fact that *clv3-2* is a strong mutation (Clark *et al.*, 1995). The effect of such severely disturbed SAM self-perpetuation on primordium geometry is that the initial bulging stage, leading to the formation of shallow crease, exhibits a variable shape. Also the adaxial primordium boundary is affected. Such effects may be attributed to the interdependence between two fundamental processes taking place at the SAM, i.e. its self-perpetuation and the formation of primordia. This interdependence may be explained by an influence of SAM geometry (physical constraints which are discussed later) or by disturbed signalling between the SAM, in particular its central zone, and the early primordium. A putative signalling from the primordium to the central SAM zone has been shown, for example, in *Petunia hybrida*, where HAIRY MERISTEM (HAR), a transcription factor encoded by a gene expressed in differentiating cells of a new primordium, is required to maintain the uncommitted state of the SAM cells. HAR is acting non-cell-autonomously, in parallel with *Petunia hybrida* WUSCHEL (Stuurman *et al.*, 2002; Carles and Fletcher, 2003). The central zone has also been postulated to influence primordia formation (Golz and Hudson, 2002; Sharma *et al.*, 2003). This is supported, for example, by the observation that, in plants where the CLV3 level is increased in the SAM (mimicking the *wus* mutation effect), putative repellence between the SAM and flower primordia is diminished (Müller *et al.*, 2006).

The effects of the *clv3-2* mutation observed later in flower primordium development are of a direct nature. They are manifested in the increased size of the primordium bulge similarly to the SAM. This results in an altered sepal number and delayed overtopping of the floral dome by sepal primordia.

Early development of the clv3-2 *flower interpreted in terms of physical constraints*

On the basis of microsurgical experiments, Mary and Roger Snow (Snow and Snow, 1947) draw the conclusion that each new leaf primordium arises in the first available space on the meristem, which is above and between the existing primordia. Prior to primordium initiation, this space needs to attain some necessary width and distance from the SAM top. Thus the determination by existing leaves of the position of the new one depends on the shape and size of the apex surface occupied by their bases (Snow and Snow, 1947, 1962), as well as of the SAM periphery. Recently, the results of the original Snows' experiments have been confirmed by the experiments of Reinhardt *et al.* (2005) in which laser ablation and modern microsurgery methods were used. The available space postulate is supported by the present observations. New primordia in *clv3-2* do not appear in an overall regular phyllotactic pattern, but occupy every wedge-shaped region available between the already formed primordia that, at the same time, are the most distant from the SAM.

A postulate on the determination of the primordium position and shape, to some extent similar to the Snows', has been put forward by Williams (1975). On the basis of quantitative analysis of the apex geometry obtained from stacks of serial transverse sections, Williams (1975) has postulated that physical constraint is an important determinant of growth at the shoot apex, and plays a role in the generation of form ('the mechanico-chemical field theory'). The putative adjustment of primordium shape and size to the physical constraints exerted by already existing primordia and the SAM periphery is apparent in various flower developmental stages of *clv3-2*, both in sequential replicas and in longitudinal sections of the apices. In addition, stereoscopic reconstruction of the apex shape reveals that the outer periclinal walls of cells located at the base of the flower axil are folded upward, as if there were buckling due to compression across the axil.

Concluding, the *clv3-2* inflorescence SAM may turn out to be a very valuable for future experiments on the role of

biomechanical factors because of the relatively easy access to the inflorescence SAM and the already observed putative significance of physical constraints. It would also be worthwhile to follow the dynamics of certain gene expression patterns so that the stages of primordium formation, like those defined by Carraro *et al.* (2006) for the wild type, could be followed. Boundary genes in particular are of interest, since boundary variation is one of the unique features of the mutant. Therefore, possible relationships between the expression patterns of these gene and mechanical factors could be also examined.

Acknowledgements

The authors thank Professor Zygmunt Hejnowicz for critical reading of this manuscript, as well as Drs Zofia Czarna and Krystyna Heller (Electron Microscopy Laboratory, Wrocław University of Environmental and Life Sciences, Poland) for help in preparing the scanning electron micrographs used in this work. TS and A-LR-K research on SAM has been financially supported by the MC-RTN EU grant SY-STEM, which also funded A-LR-K employment.

References

Arun KS, Huang TS, Blostein SD. 1987. Least-squares fitting of two 3-D point sets. *IEEE Transactions on Pattern Analysis and Machine Intelligence* **9,** 698–700.

Brand U, Fletcher JC, Hobe M, Meyerowitz EM, Simon R. 2000. Dependence of stem cell fate in *Arabidopsis* on a feedback loop regulated by *CLV3* activity. *Science* **289,** 617–619.

Buvat R. 1989. *Ontogeny, cell differentiation, and structure of vascular plants*. Berlin: Springer-Verlag.

Carles CC, Fletcher JC. 2003. Shoot apical meristem maintenance: the art of a dynamic balance. *Trends in Plants Science* **8,** 394–401.

Carraro N, Peaucelle A, Laufs P, Traas J. 2006. Cell differentiation and organ initiation at the shoot apical meristem. *Plant Molecular Biology* **60,** 811–826.

Clark SE, Running MP, Meyerowitz EM. 1993. *CLAVATA1*, a regulator of meristem and flower development in *Arabidopsis*. *Development* **119,** 397–418.

Clark SE, Running MP, Meyerowitz EM. 1995. *CLAVATA3* is a specific regulator of shoot and floral meristem development affecting the same processes as *CLAVATA1*. *Development* **121,** 2057–2067.

Crone W, Lord EM. 1993. Flower development in the organ number mutant *clavata1-1* of *Arabidopsis thaliana* (Brassicaceae). *American Journal of Botany* **80,** 1419–1426.

Dumais J, Kwiatkowska D. 2002. Analysis of surface growth in shoot apices. *The Plant Journal* **31,** 229–241.

Fletcher JC, Brand U, Running MP, Simon R, Meyerowitz EM. 1999. Signaling of cell fate decisions by *CLAVATA3* in *Arabidopsis* shoot meristem. *Science* **283,** 1911–1914.

Foster AS. 1939. Problems of structure, growth and evolution in the shoot apex of seed plants. *Botanical Reviews* **5,** 454–470.

Golz JF, Hudson A. 2002. Signalling in plant lateral organ development. *The Plant Cell* S277–S288.

Hempel FD, Feldman LJ. 1994. Bi-directional inflorescence development in *Arabidopsis thaliana*: acropetal initiation of flowers and basipetal initiation of paraclades. *Planta* **192,** 276–286.

Hepworth SR, Klenz JE, Haughn GW. 2006. UFO in the *Arabidopsis* inflorescence apex is required for floral-meristem identity and bract suppression. *Planta* **223,** 769–778.

Johansen DA. 1940. *Plant microtechnique*. New York, London: McGraw-Hill Inc.

Kayes JM, Clark SE. 1998. *CLAVATA2*, a regulator of meristem and organ development in *Arabidopsis*. *Development* **125,** 3843–3851.

Kwiatkowska D. 2004. Structural integration at the shoot apical meristem: models, measurements, and experiments. *American Journal of Botany* **91,** 1277–1293.

Kwiatkowska D. 2006. Flower primordium formation at the *Arabidopsis* shoot apex: quantitative analysis of surface geometry and growth. *Journal of Experimental Botany* **57,** 571–580.

Kwiatkowska D. 2008. Flowering and apical meristem growth dynamics. *Journal of Experimental Boany* **59,** 187–201.

Kwiatkowska D, Szczęsny T. 2004. Quantification of growth at the shoot apical meristem of *Arabidopsis*. *Proceedings of the 4th International Workshop on Functional–Structural Plant Models*. Montpellier, France: 382–385.

Laufs P, Grandjean O, Jonak C, Kiêu K, Traas J. 1998. Cellular parameters of the shoot apical meristem in *Arabidopsis*. *The Plant Cell* **10,** 1375–1389.

Laux T, Mayer KFX, Berger J, Jürgens G. 1996. The *WUSCHEL* gene is required for shoot and floral meristem integrity in *Arabidopsis*. *Development* **122,** 87–96.

Leibfried A, To JPC, Busch W, Stehling S, Kehle A, Demar M, Kieber JJ, Lohmann JU. 2005. WUSCHEL controls meristem function by direct regulation of cytokinin-inducible response regulators. *Nature* **438,** 1172–1175.

Lenhard M, Laux T. 1999. Shoot meristem formation and maintenance. *Current Opinion in Plant Biology* **2,** 44–50.

Lindsay D, Sawhney V, Bonham-Smith P. 2006. Cytokinin-induced changes in *CLAVATA1* and *WUSCHEL* expression temporally coincide with altered floral development in *Arabidopsis*. *Plant Science* **170,** 1111–1117.

Lohmann JU, Hong RL, Hobe M, Busch MA, Parcy F, Simon R, Weigel D. 2001. A molecular link between stem cell regulation and floral patterning in *Arabidopsis*. *Cell* **105,** 793–803.

Long J, Barton MK. 2000. Initiation of axillary and floral meristems in *Arabidopsis*. *Developmental Biology* **218,** 341–353.

Mayer KFX, Shoof H, Haecker A, Lenhard M, Jürgens G, Laux T. 1998. Role of *WUSCHEL* in regulating stem cell fate in the *Arabidopsis* shoot meristem. *Cell* **95,** 805–815.

Müller R, Borghi L, Kwiatkowska D, Laufs P, Simon R. 2006. Dynamic and compensatory responses of *Arabidopsis* shoot and floral meristems to *CLV3* signaling. *The Plant Cell* **18,** 1188–1198.

Müller R, Bleckmann A, Simon R. 2008. The receptor kinase CORYNE of *Arabidopsis* transmits the stem cell–limiting signal CLAVATA3 independently of CLAVATA1. *The Plant Cell* **20,** 934–946.

Ogawa M, Shinohara H, Sakagami Y, Matsubayashi Y. 2008. *Arabidopsis* CLV3 peptide directly binds CLV1 ectodomain. *Science* **319,** 249.

Reddy GV, Heisler MG, Ehrhardt DW, Meyerowitz EM. 2004. Real-time lineage analysis reveals oriented cell divisions associated with morphogenesis at the shoot apex of *Arabidopsis thaliana*. *Development* **131,** 4225–4237.

Reddy GV, Meyerowitz EM. 2005. Stem-cell homeostasis and growth dynamics can be uncoupled in the *Arabidopsis* shoot apex. *Science* **310,** 663–667.

Reinhardt D, Frenz M, Mandel T, Kuhlemeier C. 2005. Microsurgical and laser ablation analysis of leaf positioning and dorsoventral patterning in tomato. *Development* **132,** 15–26.

Romberger JA, Hejnowicz Z, Hill JF. 1993. *Plant structure: function and development*. Berlin: Springer Verlag.

Routier-Kierzkowska A-L, Kwiatkowska D. 2008. New stereoscopic reconstruction protocol for scanning electron microscope images and its application to *in vivo* replicas of the shoot apical meristem. *Functional Plant Biology* **35,** 1034–1046.

Sharma VK, Carles C, Fletcher JC. 2003. Maintenance of stem cell populations in plants. *Proceedings of the National Academy of Sciences, USA* **100,** 11823–11829.

Smyth DR, Bowman JL, Meyerowitz EM. 1990. Early flower development in *Arabidopsis*. *The Plant Cell* **2,** 755–767.

Snow M, Snow R. 1947. On the determination of leaves. *New Phytologist* **46,** 5–19.

Snow M, Snow R. 1962. A theory of the regulation of phyllotaxis based on *Lupinus albus*. *Philosophical Transactions of the Royal Society of London, Series B* **244,** 483–514.

Struik DL. 1988. *Lectures on classical differential geometry*. New York: Dover.

Stuurman J, Jäggi F, Kuhlemeier C. 2002. Shoot meristem maintenance is controlled by a *GRAS*-gene mediated signal from differentiating cells. *Genes and Development* **16,** 2213–2218.

Traas J, Doonan JH. 2001. Cellular basis of shoot apical meristem development. *International Review of Cytology* **208,** 161–206.

Vaughan JG. 1955. The morphology and growth of the vegetative and reproductive apices of *Arabidopsis thaliana* (L.) Heynh., *Capsella bursa-pastoris* (L.) Medic. and *Anagallis arvensis* L. *Journal of the Linnean Society, London (Botany)* **55,** 279–301.

Williams MH. 1991. A sequential study of cell divisions and expansion patterns on a single developing shoot apex of *Vinca major*. *Annals of Botany* **68,** 541–546.

Williams MH, Green PB. 1988. Sequential scanning electron microscopy of a growing plant meristem. *Protoplasma* **147,** 77–79.

Williams RF. 1975. *The shoot apex and leaf growth*. New York: Cambridge University Press.